Original Article

Dose-Response:
An International Journal
July-September 2020:1-8

DOI: 10.1177/1559325820929555
journals.sagepub.com/home/dos
SAGE

A Novel Fabrication of Dose-Dependent Injectable Curcumin Biocomposite Hydrogel System Anesthetic Delivery Method for Care and Management of Musculoskeletal Pain

Xuehong Jiang[1,2], Shuaishuai Wang[1,2], and Hui Chen[1,2]

Abstract

Chronic musculoskeletal pain has biological, psychological, and social components. In this article, we have demonstrated the easily injectable nanocomposite carrier for the treatment of chronic musculoskeletal pain. Briefly, the curcumin (Cur) loaded with lipid nanocapsules (LNCs; Cur@LNCs) using the phase invasion method. The synthesized Cur@LNCs were characterized by using scanning electron microscopy, transmittance electron microscopy, and the size of the fabricated nanoparticles confirmed by dynamic light scattering analysis. The synthesized Cur@LNC injectable hydrogel shows excellent results in vivo in the rat model. We have examined the efficiency of the chronic constriction injury in the rat model and induced the pain using thermal paw withdrawal latency. The injectable hydrogels Cur@LNCs display a remarkable reduction in pain 7 days post administrations compared to the untreated group animals. This work could establish the preclinical candidate of the neuropathic pain response in the future.

Keywords

injectable nanocomposition, lipid nanocapsules, anesthetic delivery, musculoskeletal pain

Introduction

In China, more than 40 million people are disabled due to musculoskeletal pain, with a health treatment cost of more than a billion dollars. In clinical treatment, indications usually described are tenacious pain, sensitivity, marginal nerve annoyance, faintness, and incomplete gesture. The pathophysiology of musculoskeletal pain is not completely unstated, though, irritation, fibrosis, tissue poverty, and neurotransmitters as well as neurosensory turbulences have been expected to be related to the musculoskeletal pain.[1-5] Various treatments such as opioids, nonsteroidal anti-inflammatory drugs, or corticosteroids are measured as the type of maintenance for the pre- and postoperative and neuropathic management of pain.[6] However, administration with long-term opioids for precancer pain is static contentious. In this manner, the acute and chronic systematic administration of the nonsteroidal anti-inflammatory drugs was used to manage gastrointestinal and hematology toxicity, with exact inhibition of the enzymes through the nonsteroidal anti-inflammatory drugs.[7-10] The systematic inflammatory treatments for pain management have been associated with wound closure. Also, nonsteroidal anti-inflammatory drugs show some remarkable side effects, and utilization of anesthesia such as ropivacaine, curcumin, lidocaine, and bupivacaine increases the important attention as they can be managed nearby for quick action.[11-14]

To overcome the auspicious method, native anesthesia need incessant brew or numerous managements to attain the wanted

[1] Department of General Medicine, First People's Hospital of Wenling, Wenling, China
[2] Department of Spinal Surgery, First People's Hospital of Wenling, Wenling, China

Received 3 April 2020; received revised 28 April 2020; accepted 30 April 2020

Corresponding Author:
Hui Chen, Department of General Medicine, First People's Hospital of Wenling, No. 333, Chuan'an South Road, Wenling 317500, Zhejiang Province, China.
Email: hui.c34@yahoo.com

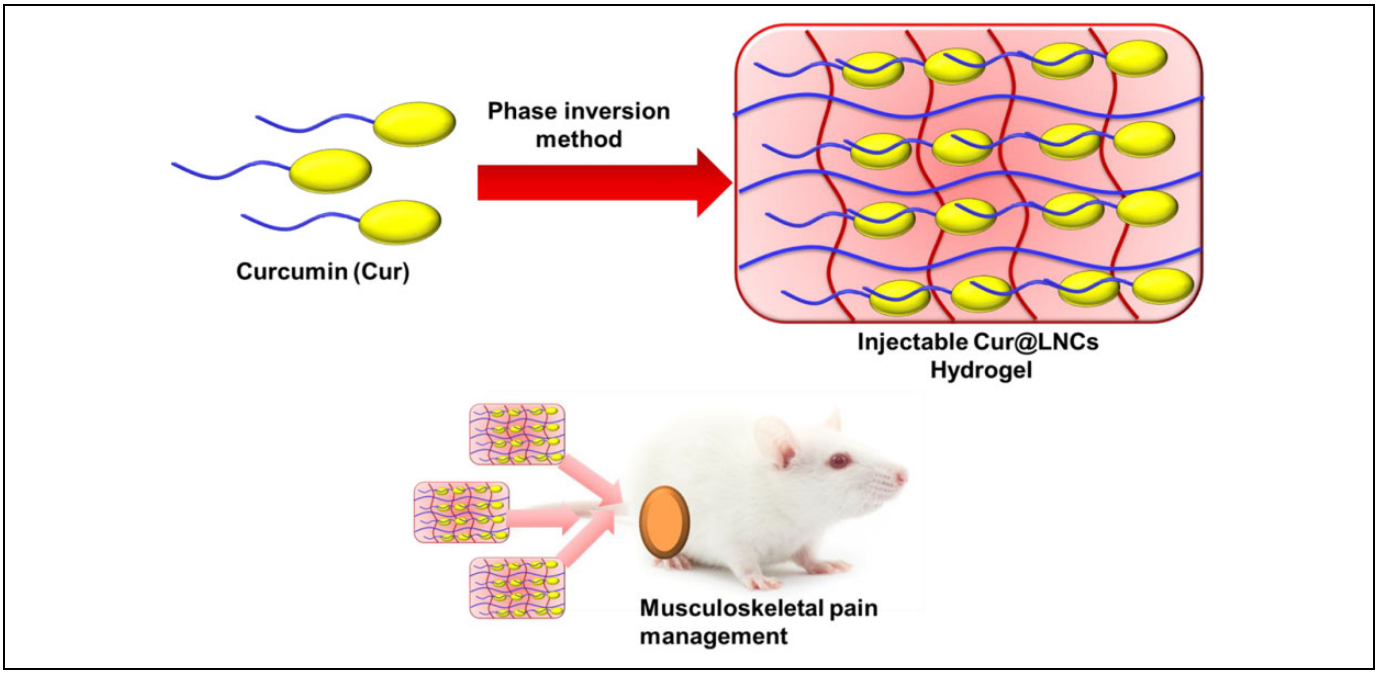

Figure 1. Graphic representation of injectable curcumin-loaded lipid nanocapsules (Cur@LNCs) hydrogel for musculoskeletal pain management.

pain respite which in the shot can lead to considerable organs response and common toxicity.[15] Consequently, the improvement in the exclusive distribution frameworks, than can remember those particles protracted period close by, can suggestively improve the efficiency, provide the sustained analgesic effects, and reduce the periods of injection connecting with side effects.[16-19] Several attempts have been made to achieve sustain transporter of local anesthesia using biocompatibility nanomaterial, for example, nanoparticles and hydrogels, to develop the nanoformulated curcumin using liposomes. The low encapsulation efficacy and debauched release the drug accumulations of the disadvantages of the carrier.[20-22] Also, recently, Polyethylene glycol (PEG)-coated curcumin shows a significant possibility. With all these advantages of the curcumin, nanoparticles could be directly injected to the patients with any form of injection to reduce the importance of the local drug.[23-25]

A natural plant of the curcumin polyphenol compounds, extracted from the turmeric plants which are easily available in Asian regions, is mainly used for pharmacological purposes. The curcumin shows excellent antioxidant property, such as anti-inflammatory, antifungus, and antitumor, and so on.[26-28] It is additionally used for the septic, digestive, and cardiovascular diseases. However, most of the therapeutic agents and biological efficient compounds are fictional to have less solubility in water; are obscure to be orally metabolic in human, with these uses of curcumin in the pharmacological field; and are owed to the less aqueous solubility, at presystematics absorption and less biodistribution.[29-31] Despite these examples, enhancing the water solubility for oral administration becomes a vital role. More recently, researchers are developed to encapsulate various strategies, such as liposome, emulsions, and hydrogels, with various polymeric materials. Also it is highly active without any side effects.[32-34]

Easily injectable hydrogels are excellent invasive drug carriers. Numerous reports have been examined regarding the different uses of tissue engineering growth for chemotherapy. Nair et al reported the chitosan-coated nanoparticles are the linear polysaccharide merged acetylated systems.[35] The drug loading capacity and the thermal framework showed numerous strategies and established in vivo efficiency for only up to 48 hours in mice blockage frame. In all these advantages, injectable hydrogel as an enzyme and drug delivery is the most important.[36-39] To this model, we combine injectable hydrogels with various nanoparticles and minimum delivery of invasive and retention of injectable hydrogels. Also, using lipid nanocapsules (LNCs) incorporated with injectable hydrogels display high encapsulated efficiency. These dynamic crosslinking associated with the easily injectable gelation of high-delivery nanoparticles were suitable for the exact pharmacological uses. With all the overall motivating points, we have constructed the injectable hydrogel loaded with the curcumin nanoparticles, which will lead to stable anesthetic pains in vivo in the rat chronic constriction injury model of pain management (Figure 1).

Materials and Methods

Preparation of Curcumin-Loaded Lipid Nanocapsules

The phase inversion method is used to prepare the LNCs bearing 100 nm size. The oil phase was immersed with the Kolliphor, Lipoid, NaCl, and Double distilled (DD) water (40%, 12.4%, 3%, 1.8%, and 43%, respectively). The solution

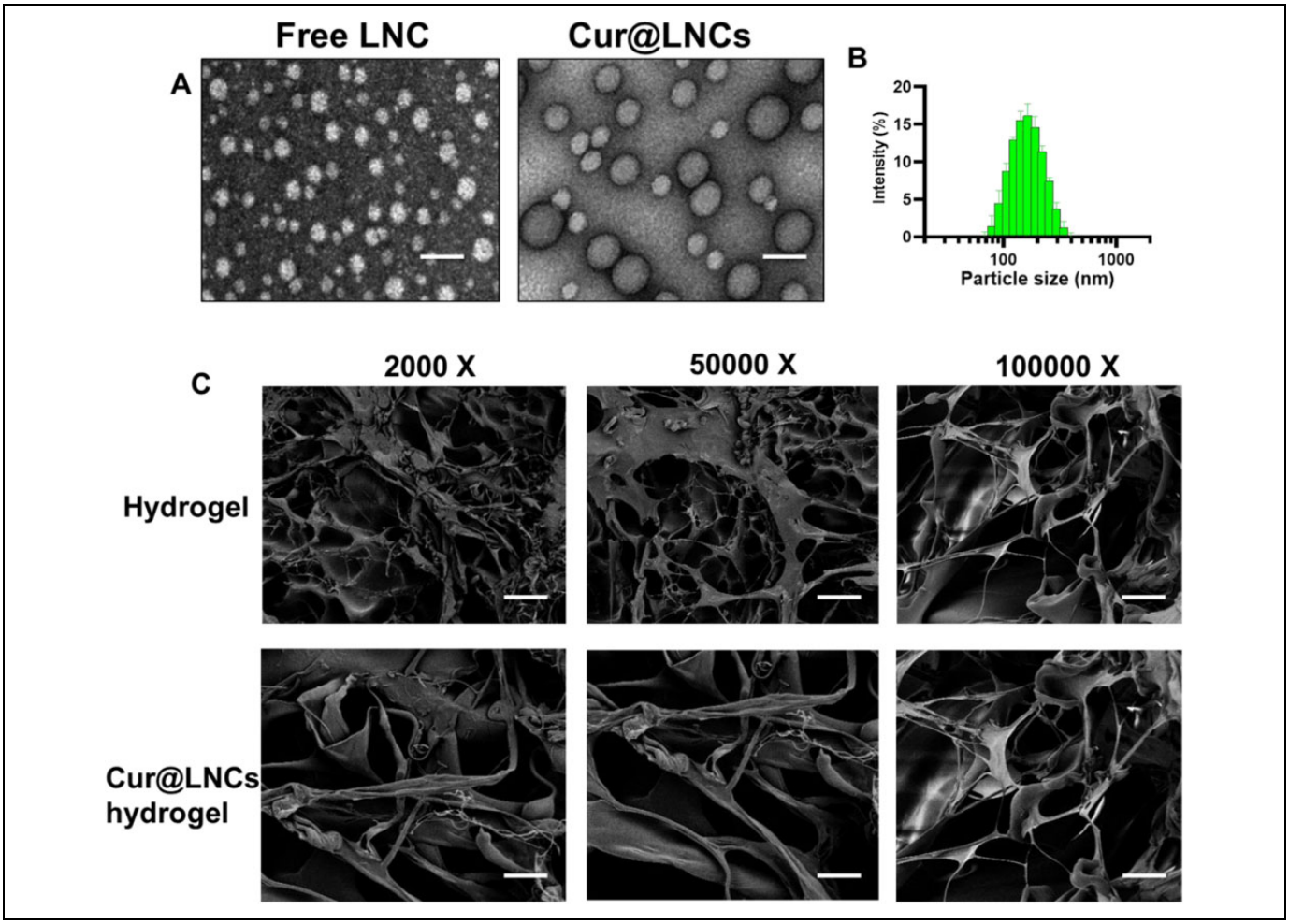

Figure 2. A, Transmission electron microscopy (TEM) descriptions of free LNC and Cur@LNCs. Scale bar 100 nm. B, Size distribution of Cur@LNCs. C, Scanning electron microscopy (SEM) descriptions of hydrogel and Cur@LNCs hydrogel composition with various magnifications.

was heated at 100 °C using a magnetic stirrer. After 5 hours, the mixture was slowly cooled at the room temperature, then 4 mL of DD water was added into the same solutions, and the same mixture was cooled for 15 minutes at room temperature.[40-43]

Characterization of the Cur@LNCs

Scanning electron microscopy (SEM) was used to detect the morphology of the hydrogel samples. The hydrogel samples were freeze-dried and coated with a 20 nm layer of gold using a sputter coater. Test samples were blown clean using trampled air before SEM characterization. The hydrodynamic diameters, ζ potentials, and polydispersity indexes (PDIs) of free LNCs and Cur@LNCs were measured by dynamic light scattering (DLS) on a Malvern Nano-ZS90 instrument (Malvern Instruments) at 25 °C. TECNAL 10 (Philips) was used to obtain transmission electron microscopy (TEM) images, operating at an acceleration voltage of 80 kV. Nanoparticles at a concentration with free LNCs and Cur@LNCs were placed onto a 300-mesh copper grid coated with carbon. Approximately 2 minutes after deposition, the surface water was removed with filter paper and then air-dried. Positive staining was performed using a 2 wt% aqueous uranyl acetate solution.

In Vitro Curcumin Release From the Cur@LNCs Hydrogels

The release profiles of total curcumin and Cur@LNCs were monitored by dialysis using a membrane (Spectrum Laboratories, molecular weight cutoff 14 kDa). Briefly, 10 mL of Cur@LNCs hydrogels (0.1 mg/mL curcumin or Cur@LNCs equivalent concentration) were dialyzed against 40 mL of phosphate-buffered solutions (pH 7.4, 0.2% Tween 80) at 37 °C. At predetermined time intervals, the release media (1 mL) were collected, and the fresh media (1 mL) were supplemented.

In Vivo Examinations of the Cur@LNCs

The female Sprague Dawley (SD) rats weigh around 250 to 300 g. Totally, 10 mice and 20 rats were used for this examination. Care and animal experimental procedures were followed according to the guidelines provided by the approved

Institutional Animal Care and Use Committee of Department of General Medicine, First People's Hospital of Wenling, Wenling, China. The mice and rats were separately housed 3 per cage, maintained at room temperature and atmospheric conditions.

Chronic Constrictions Injury of the Sciatic Nerves

The chronic constrictions injury (CCI) was surgically triggered on the right hind limb of the SD rats as described in previously reported protocol.[44,45] The animals were anesthetized with 4% chloroform for initiation for maintenance. A 15 mm of skin incitation was created via rounded partitions of the biceps of the female muscles. More or less 8 to 10 mm of the right sciatic nerves was unfettered surrounding soft organs. Four 4-0 Vicryl sutures were tied loosely. The LNC hydrogels were injected through the mice's muscle layer. The animals were with special care and without weight loss, which were monitored every day 3 days postadministration. The rats were separated into 3 groups (n = 5, n is the number of mice). Group 1 was without treatment (untreated, bearing cranial cruciate ligament (CCL) only). Group 2 was LNC hydrogel without curcumin (free 0.3 GC + LNCs). Group 3 was Cur@LNCs (0.3 GC + Cur@LNCs). The 400 μL of the saline and drugs were injected for each rat.

Examinations of Thermal Hyperalgesia Response via Neurobehavior

To examine the efficiency of the treatment with hypersensitivity of the hot plate was used as previously defined with amendments. Beforehand the CCL, rats were adapted for 3 days to examine and monitor the baseline heat plate withdrawal latency as displayed. The surgeries with pre- and postadministration with various time points were examined. The time points are 6, 24, 36, 48, 72, 84, 96, 108, 120, 132, 144, and 168 hours. The initial 1 to 5 days was examining each per day. The assessment conducted before the surgery (0 hour) served as the standard matrix.

CCL Tissue Collections and Histology Examinations

Aimed at the histological examinations, animals were killed after 1 week of surgery using aspirin. The surgical place was unlocked and unprotected to assess any ciphers of uncultured pathology. The sciatic nerves and surroundings with and without tissues were obtained from the injection place. The harvested tissue was secured in the 10% buffer formalin for 48 hours. Later, the tissue was cleaned with saline and fixed in 4% formaldehyde. Then, we prepared the tissues for hematoxylin and eosin (H&E) for staining purposes.[46-48]

Statistical Analysis

The statistics are obtainable as means ± SD. The meaning of the associated examinations was assessed by 2-tailed unpaired Student *t* test. All analyses were achieved with GraphPad Prism statistics 17.0 (*$P < .05$; **$P < .01$; ***$P < .001$).

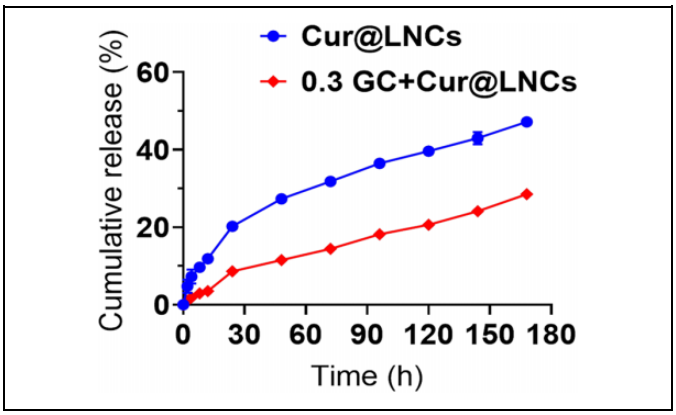

Figure 3. Curcumin release form LNCs (Cur@LNCs) with 0.3 GC and Cur@LNCs analyzed through the Reversed-phase High-performance Liquid Chromatography (RP-HPLC). Eruption release of curcumin was examined first 3 hours and subsequent release of curcumin shown remarkable decrease in 0.3 GC and Cur@LNCs composition associated with the Cur@LNCs.

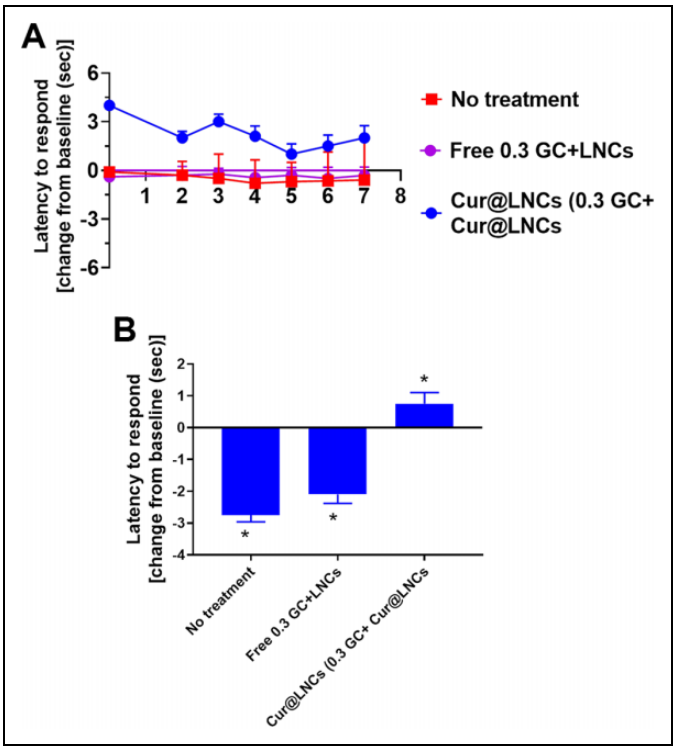

Figure 4. A, Image of the thermal withdrawal potential up to 7 days postadministration. B, Normal response displays through various examinations groups. Graphs stated as mean ± standard error of the mean (SEM). Error bar designate a 95% CI ($P < .05$).

Results and Discussions

Synthesis, Characterization, and Morphology of Cur@LNC Hydrogels

The LNC hydrogels were prepared according to the phase inversion process using Labrafac lipid. The compounds are

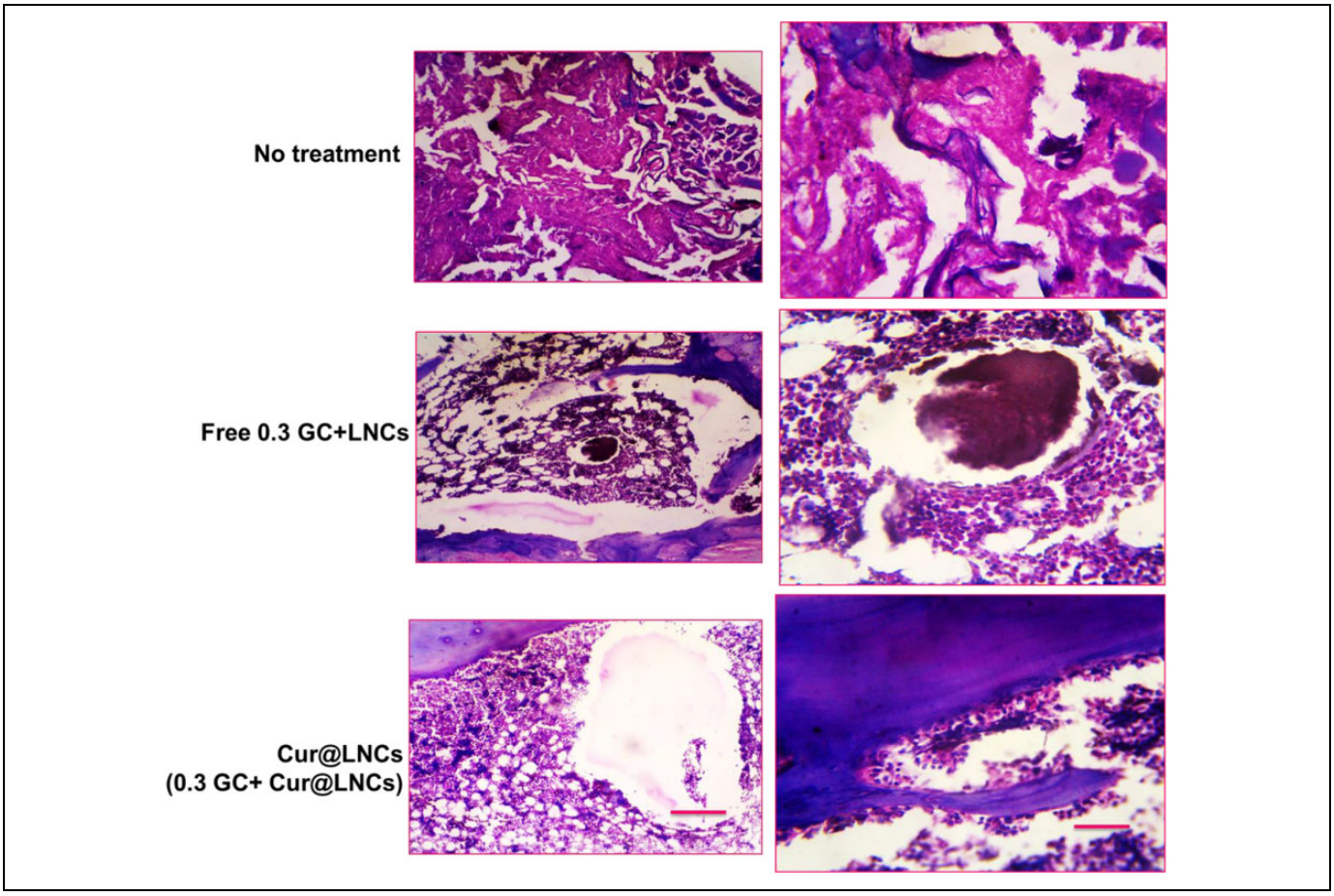

Figure 5. Optical microscopic representations of hematoxylin and eosin stain pieces of the nearby sciatic nerves for various treatments. Black around image scale bar = 100 μm.

used at the exact concentration to prepare the nanocapsule hydrogels of around ~100 nm size with various drug loading and free LNC hydrogels. The dual drug loading and free LNC hydrogels displayed the exact diameters indicating a low PDI index (<0.200). The exact spherical metrology was examined through the TEM analysis (Figure 2A). Further, the encapsulation efficacy of curcumin with various concentrations in Cur@LNCs hydrogels. The 1.0%, 1.5%, and 2.0% amounts of drug-loaded composition; 95%, 91%, and 75% of EE; and 1.19%, 1.38%, and 1.79% (wt/wt) of drug loading, respectively. As shown in Figure 2B, Cur@LNCs presented small and sphere particles. Compared with free LNC, Cur@LNCs was more uniform and dispersive.

The Cur@LNCs hydrogels were invented via immersion of LNC interruption with 0.3 GC polymeric solution and the solution was cross-linked using horseradish peroxidase (HRP) and hydrogen peroxide (H_2O_2). The hydrogenation of the LNC hydrogels was obtained to be dependent on the portion of the LNCs and the polymeric as well as the ratio of the H_2O_2 and HRP. The ratio of H_2O_2 and HRP was enhanced to accomplish the clinically feasible hydrogenation periods of 50 seconds. The SEM displays the SEM of LNCs hydrogels and Cur@LNCs hydrogels. The SEM analysis indicates the formation of the Cur@LNCs hydrogels within the matrix shows the clear spherical round morphology in the hydrogels (Figure 2C).

In Vitro Curcumin Release From the Cur@LNC Hydrogels

After the combination of the Cur@LNC hydrogels with the PEG matrix through the nanoprecipitation to form curcumin-polymer nanocomposites. We assessed curcumin release from the respective Cur@LNCs. Probably, Cur@LNCs exhibited enhanced drug retention within PEG matrices (Figure 3). Intriguingly, Cur@LNCs exhibited a faster rate of the kinetics. In sharp contrast, only a negligible amount of 3 (~10%) was liberated after incubation for 4 days.

In Vivo Examinations of CCL Rat Model for Cur@LNC Hydrogels

The potential to the response of the represented TWL in the baseline condition is shown in Figure 4 for the predetermined period. Also, the regular reply displayed in every treated group. But the medication release examinations show the medication

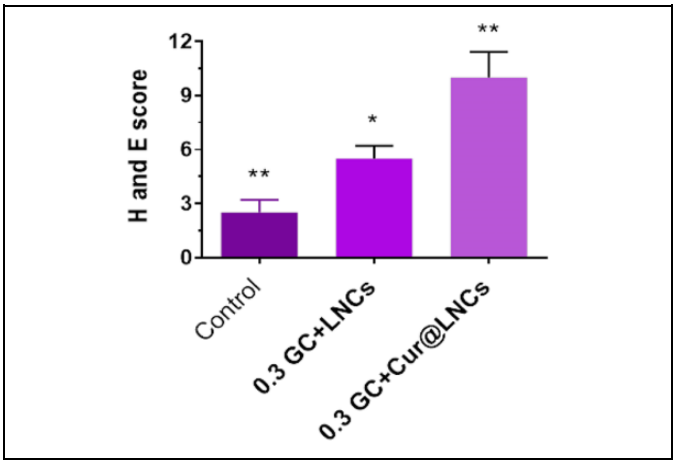

Figure 6. Hematoxylin and eosin scores of the control (no treatment), 0.3 GC + LNCs, and 0.3 GC + Cur@LNCs groups.

proportions were used in these examinations to enhance the gel medication loadings. Further, the sensory obstruction was monitored to enhance TWL from the initial stage. The nontreated groups go with the surgery with less biomaterials focused at the place of nerve constriction damage. Also, the nontreated groups show the low TWL for the sciatic nerve damages. Group 2 shows the effects of the free (0.3 GC + LNCs) show without entrenched in the hydrogels. Finally, group 3 was Cur@LNCs (0.3 GC + Cur@LNCs) and enhanced TWL and attenuated the heat hyperalgesia, and the animals are used in each. All the animals of these groups displayed the important sensory obstruction in all 7 days of the time. Furthermore, the average animal treated with different environments in 7 days was evaluated via the average of all the animal behaviors in these groups. The ratio of the animals was examined statically with 0.3 GC + Cur@LNCs and without treatment. The in vivo examination outcomes suggested that the transporter of the curcumin-loaded injectable hydrogels of LNCs for nanocomposites is cheap and active in the injury produced by thermal hyperalgesia.

Muscle Tissues and Biocompatibility Examinations

The sciatic nerves and the nearby places of the muscle tissue of the animals were gathered at the end of the 7 days postadministration to endorse the detail of the reaction of the tissue. Each group's tissues were used for these examinations with reliable outcomes in all tissue samples. All the samples were examined by H&E and histological evaluations were conducted as shown in Figure 5. The nontreated groups (healthy animals) show any inflammations in the surface of the animals. The nerve also fails to show the inflammations and cover was complete, suggesting that the compressions did not injure the nerve and were individual accountable for encouraging pain, as intended. Also, the muscles and the tissues nearby the nerves were regular without any damages. In free 0.3 GC + LNCs, the establishment displays the remarkable cell infiltration shown by the cells of macrophages, neutrophils, phagocytic, and the lymphocytes. Also, the 0.3 GC + Cur@LNCs animal groups show the hydrogels significantly reduce the damages by showing any other tissue damages. Besides these groups show no marks of the acute systematic toxicity or injury of nerves at the nearby established place.

The H&E score was higher in the 0.3 GC + LNCs group when compared with that in the control group (Figure 6). Furthermore, the score was greater in the 0.3 GC + Cur@LNC ($P < .05$) and 12-hour ($P < .05$) groups compared with that in the 0.3 GC + LNCs group, and it increased further at 0.3 GC + Cur@LNCs.

Conclusions

The musculoskeletal postoperative disadvantages display the nonstop brew or numerous indigenous inoculations of native analgesics. In this work, we have established the synthesis of Cur@LNCs developed by the phase inversion methods. The Cur@LNCs were characterized by various electroscopic methods and the size was confirmed by the DLS analysis. The nanocomposites for the transporter for the CCI model. Also, it can reduce the pain sense to baseline of within 7 days. The reduced heat hyperalgesia used to evaluate the Cur@LNCs for the preclinical uses to treatment postoperation, musculoskeletal and for the all pain management purposes in future.

Declaration of Conflicting Interests

The author(s) declared no potential conflicts of interest with respect to the research, authorship, and/or publication of this article.

Funding

The author(s) received no financial support for the research, authorship, and/or publication of this article.

ORCID iD

Hui Chen https://orcid.org/0000-0001-6325-3521

Supplemental Material

Supplemental material for this article is available online.

References

1. Salathé CR, Kälin W, Zilse S, Elfering A. Baseline musculoskeletal pain and impaired sleep related to school pressure influence the development of musculoskeletal pain in N = 107 adolescents in a 5-year longitudinal study. *Eur Spine J*. 2020;29(3):540-548. doi:10.1007/s00586-019-06211-x
2. Amorim RAR, Moreira GA, Santos FH, et al. Sleep and restless legs syndrome in female adolescents with idiopathic musculoskeletal pain. *J Pediatr*. 2019:pii: S0021–7557(19)30123–8. doi:10.1016/j.jped.2019.09.007
3. Tabaku SB, Gupta R, Jenkins TM, et al. Musculoskeletal pain, physical function, and quality of life after bariatric surgery. *Pediatrics*. 2019;144(6):pii: e20191399. doi:10.1542/peds.2019-1399

4. Lentz TA, Goode AP, Thigpen CA, George SZ. Value-based care for musculoskeletal pain: are physical therapists ready to deliver? *Phys Ther*. 2020;100(4):621-632. doi:10.1093/ptj/pzz171
5. Lentz TA, Harman JS, Marlow NM, Beneciuk JM, Fillingim RB, George SZ. Factors associated with persistently high-cost health care utilization for musculoskeletal pain. *PLoS One*. 2019;14(11): e0225125. doi:10.1371/journal.pone.0225125
6. Shang ZP, Xu LL, Lu YY, et al. Advances in chemical constituents and quality control of turmeric. *World J Tradit Chin Med*. 2019;5(2):116-121. doi:10.4103/wjtcm.wjtcm_12_19
7. Norheim KL, Samani A, Bonlokke JH, Omland O, Madeleine P. On the role of ageing and musculoskeletal pain on dynamic balance in manual workers. *J Electromyogr Kines*. 2019;50:102374. doi:10.1016/j.jelekin.2019.102374
8. Marinangeli F, Evangelista M, Finco G. Tapentadol prolonged release in the treatment of musculoskeletal pain: an innovative pharmacological option. *Eur Rev Med Pharmacol Sci*. 2019; 23(4 suppl):5-13. doi:10.26355/eurrev_201911_19378
9. Marklund S, Mienna CS, Wahlström J, Englund E, Wiesinger B. Work ability and productivity among dentists: associations with musculoskeletal pain, stress, and sleep. *Int Arch Occup Environ Health*. 2019;93(2):271-278. doi:10.1007/s00420-019-01478-5
10. Neupane S, Lallukka T, Pietiläinen O, Rahkonen O, Arjas PL. Trajectories of multisite musculoskeletal pain in midlife: associations with common mental disorders. *Eur J Pain*. 2019;24(2): 364-373. doi:10.1002/ejp.1492
11. Hashkes PJ. Will resilience give hope to youth with chronic musculoskeletal pain? *J Pediatr*. 2019;210:1-2. doi:10.1016/j.jpeds. 2019.05.010
12. Barbero M, Schneebeli A, Koetsier E, Maino P. Myofascial pain syndrome and trigger points: evaluation and treatment in patients with musculoskeletal pain. *Curr Opin Support Palliat Care*. 2019; 13(3):270-276. doi:10.1097/spc.0000000000000445
13. Tsepilov Y, Freidin M, Shadrina AS, et al. Analysis of genetically independent phenotypes identifies shared genetic factors associated with chronic musculoskeletal pain at different anatomic sites. *Biorxiv*. 2019. doi:10.1101/810283
14. Rapolienė L, Razbadauskas A, Mockevičienė D, Varžaitytė L, Skarbalienė A. Balneotherapy for musculoskeletal pain: does the mineral content matter? *Int J Biometeorol*. 2019. doi:10.1007/ s00484-019-01800-3
15. Wang J, Wan Y. Acupuncture mechanisms: anesthesia, analgesia and protection on organ functions. *World J Tradit Chin Med*. 2015;1(1):59-66.
16. Mohiuddin OA, Campbell B, Poche JN, et al. Decellularized adipose tissue hydrogel promotes bone regeneration in critical-sized mouse femoral defect model. *Front Bioeng Biotechnol*. 2019;7: 211. doi:10.3389/fbioe.2019.00211
17. Kursumovic A, Muir JM, Ammerman J, Bostelmann R. The disability cascade: a preventable consequence of the loss of disc height following lumbar microdiscectomy. *Cureus*. 2019;11(7): e5169. doi:10.7759/cureus.5169
18. Tendulkar G, Chen T, Ehnert S, Kaps HP, Nüssler AK. Intervertebral disc nucleus repair: hype or hope? *Int J Mol Sci*. 2019; 20(15):pii: E3622. doi:10.3390/ijms20153622
19. Khanal M, Gohil VS, Kuyinu E, et al. Injectable nanocomposite analgesic delivery system for musculoskeletal pain management. *Acta Biomater*. 2018;74:280-290. doi:10.1016/j.actbio. 2018.05.038
20. Hsiao MY, Lin AC, Liao WH, et al. Dug-loaded hyaluronic acid hydrogel as a sustained-release regimen with dual effects in early intervention of tendinopathy. *Sci Rep*. 2019;9(1):4784. doi:10.1038/s41598-019-41410-y
21. Casanellas I, Lizarribar AG, Lagunas A, Samitier J. Producing 3D biomimetic nanomaterials for musculoskeletal system regeneration. *Front Bioeng Biotechnol*. 2018;6:128. doi:10.3389/fbioe. 2018.00128
22. Hom WW, Tschopp M, Lin HA, et al. Composite biomaterial repair strategy to restore biomechanical function and reduce herniation risk in an ex vivo large animal model of intervertebral disc herniation with varying injury severity. *PloS One*. 2019;14(5): e0217357. doi:10.1371/journal.pone.0217357
23. Zhao D, Chen Z, Hu S, et al. Efficacy and safety of loxoprofen hydrogel transdermal patch versus loxoprofen tablet in Chinese patients with myalgia: a double-blind, double-dummy, parallel-group, randomized, controlled, non-inferiority trial. *Clin Drug Investig*. 2019;39(4):369-377. doi:10.1007/s40261-019-00756-x
24. Wells CM, Harris M, Choi L, Murali VP, Guerra FD, Jennings JA. Stimuli-responsive drug release from smart polymers. *J Funct Biomater*. 2019;10(3):pii: E34. doi:10.3390/jfb10030034
25. Imada M, Yagyuu T, Ueyama Y, et al. Prevention of tooth extraction-triggered bisphosphonate-related osteonecrosis of the jaws with basic fibroblast growth factor: an experimental study in rats. *PloS One*. 2019;14:e0211928. doi:10.1371/journal.pone. 0211928
26. Kamar SS, Abdel Kader DH, Rashed LA. Beneficial effect of curcumin nanoparticles-hydrogel on excisional skin wound healing in type-i diabetic rat: histological and immunohistochemical studies. *Ann Anat*. 2019;222(2019):94-102. doi:10.1016/j.aanat. 2018.11.005
27. He F, Jiao H, Tian Y, et al. Facile and large-scale synthesis of curcumin/PVA hydrogel: effectively kill bacteria and accelerate cutaneous wound healing in the rat. *J Biomater Sci Polym Ed*. 2018;29(4):325-343. doi:10.1080/09205063. 2017.1417002
28. Chen G, Li J, Cai Y, et al. A glycyrrhetinic acid-modified curcumin supramolecular hydrogel for liver tumor targeting therapy. *Sci Rep*. 2017;7:44210. doi:10.1038/srep44210
29. Lu C. Reversal of oxidative stress in neural cells by an injectable curcumin/thermosensitive hydrogel. *Curr Drug Deliv*. 2016; 13(5):682-687. doi:10.2174/1567201813666151109102532
30. Qi XJ, Liu XY, Tang LM, Li PF, Qiu F, Yang AH. Antidepressant effect of curcumin-loaded guanidine-chitosan thermo-sensitive hydrogel by nasal delivery. *Pharm Dev Technol*. 2019;25(3):316-325. doi:10.1080/10837450.2019.1686524
31. Teong B, Lin CY, Chang SJ. Enhanced anti-cancer activity by curcumin-loaded hydrogel nanoparticle derived aggregates on A549 lung adenocarcinoma cells. *J Mater Sci Mater Med*. 2015;26(1):5357. doi:10.1007/s10856-014-5357-3
32. Banerjee SL, Samanta S, Sarkar S, Singha NK. A self-healable and antifouling hydrogel based on PDMS centered ABA tri-block

copolymer polymersomes: a potential material for therapeutic contact lenses. *J Materials Chem B*. 2019;8(2):226-243. doi:10.1039/c9tb00949c

33. Bhattacharya D, Tiwari R, Bhatia T, et al. Accelerated and scarless wound repair by a multicomponent hydrogel through simultaneous activation of multiple pathways. *Drug Deliv Transl Res*.2019;9(6):1143-1158. doi:10.1007/s13346-019-00660-z
34. George D, Maheswari PU, Sheriffa Begum KMM, Arthanareeswaran G. Biomass-derived dialdehyde cellulose cross-linked chitosan-based nanocomposite hydrogel with phytosynthesized zinc oxide nanoparticles for enhanced curcumin delivery and bioactivity. *J Agric Food Chem*. 2019;67(39):10880-10890. doi:10.1021/acs.jafc.9b01933
35. Foley PL, Ulery BD, Kan HM, et al. A chitosan thermogel for delivery of ropivacaine in regional musculoskeletal anesthesia. *Biomaterials*. 2013;34(10):2539-2546. doi:10.1016/j.biomaterials.2012.12.035
36. Vollono L, Falconi M, Gaziano R, et al. Potential of curcumin in skin disorders. *Nutrients*. 2019;11(9):pii: E2169. doi:10.3390/nu11092169
37. Xu J, Liu Y, Hsu SH. Hydrogels based on Schiff base linkages for biomedical applications. *Molecules*. 2019;24(16):pii: E3005. doi:10.3390/molecules24163005
38. Scuto MC, Mancuso C, Tomasello B, et al. Curcumin, hormesis and the nervous system. *Nutrients*. 2019;11(10):2417. doi:10.3390/nu11102417
39. Gao C, Liu L, Zhou Y, Bian Z, Wang S, Wang Y. Novel drug delivery systems of Chinese medicine for the treatment of inflammatory bowel disease. *Chin Med*. 2019;14:23. doi:10.1186/s13020-019-0245-x
40. Abbasi Z, Shamsaei E, Fang XY, Ladewig B, Wang H. Simple fabrication of zeolitic imidazolate framework ZIF-8/polymer composite beads by phase inversion method for efficient oil sorption. *J Colloid Interface Sci*. 2017;493:150-161. doi:10.1016/j.jcis.2017.01.006
41. Tao MM, Liu F, Xue XL. Poly(vinylidene fluoride) membranes by an ultrasound assisted phase inversion method. *Ultrason Sonochem*. 2013;20(1):232-238. doi:10.1016/j.ultsonch.2012.08.013
42. Biouki MH, Mobedi H, Karkhaneh A, Joupari MD. Development of a simvastatin loaded injectable porous scaffold in situ formed by phase inversion method for bone tissue regeneration. *Int J Artif Organs*. 2019;42(2):72-79. doi:10.1177/0391398818806161
43. Hua X, Ding P, Wang M, Chi K, Yang R, Cao Y. Emulsions prepared by ultrahigh methoxylated pectin through the phase inversion method. *Int J Biol Macromol*. 2019;128:167-175. doi:10.1016/j.ijbiomac.2019.01.111
44. Cao S, Yuan J, Zhang D, Wen S, Wang J, Li Y, Deng W. Transcriptome changes in dorsal spinal cord of rats with neuropathic pain. *J Pain Res*. 2019;12:3013-3023. doi:10.2147/jpr.s219084
45. Melkani I, Kumar B, Panchal S, et al. Comparison of sildenafil, fluoxetine and its co-administration against chronic constriction injury induced neuropathic pain in rats: an influential additive effect. *Neurol Res*. 2019;41(10):875-882. doi:10.1080/01616412.2019.1630091
46. Tan CY, Wang YP, Han YY, et al. Expression and effect of sodium-potassium-chloride cotransporter on dorsal root ganglion neurons in a rat model of chronic constriction injury. *Neural Regen Res*. 2020;15(5):912-921. doi:10.4103/1673-5374.268904
47. Stevens AM, Liu L, Bertovich D, Janjic JM, Pollock JA. Differential expression of neuroinflammatory mRNAs in the rat sciatic nerve following chronic constriction injury and pain-relieving nanoemulsion NSAID delivery to infiltrating macrophages. *Int J Mol Sci*. 2019;20(21):pii: E5269. doi:10.3390/ijms20215269
48. Li Y, Li H, Han J. Sphingosine-1-phosphate receptor 2 modulates pain sensitivity by suppressing the ROS-RUNX3 pathway in a rat model of neuropathy. *J Cell Physiol*. 2019;235(4):3864-3873. doi:10.1002/jcp.29280